Contactless Measurement of Heart Rate Variability from Pupillary Fluctuations

Avinash Parnandi and Ricardo Gutierrez-Osuna
Department of Computer Science and Engineering
Texas A&M University
College Station, TX 77840, USA
{parnandi, rgutier}@tamu.edu

***Abstract*— The ability to measure a person's physiological parameters in a contactless fashion (i.e., without attaching electrodes to the skin) has tremendous potential in a number of applications, from affective interfaces to healthcare delivery. In this paper, we present a proof-of-concept method for measuring one such vital parameter, heart rate variability (HRV), in a contactless fashion from spontaneous fluctuations in pupillary diameter. Our approach uses a remote eye tracker for imaging and an integro-differential algorithm for segmenting the pupil-iris boundary. We then estimate HRV from the relative distribution of energy in the low frequency (0.04 to 0.15 Hz) and high frequency (0.15 to 0.4 Hz) bands of the power spectrum of the time series of pupillary fluctuations. We validated the method under a range of breathing conditions and under different illumination levels. Our results show a high degree of agreement between our pupillary estimate of HRV and ground truth measurements from an ECG-grade heart rate monitor. These results support the feasibility of estimating HRV in a non-contact, non-invasive fashion.**

Keywords— Contactless sensors, physiological sensing, heart rate variability, pupillometry.

I. INTRODUCTION

Physiological parameters provide important information on the health, emotional, and cognitive state of a person. Parameters such inter beat interval (IBI), heart rate variability (HRV) or electro-dermal activity (EDA) are all indicators of modulation in the autonomic nervous system (ANS) [1]. Physiological signals are also widely used for health and fitness monitoring, stress assessment, affective computing, psychophysiological studies, and a multitude of other applications. Among the different physiological variables, HRV is of special significance because it provides important information about cardiovascular regulation, and for the diagnosis of cardiac and other chronic diseases [2].

However, HRV measurement with existing technologies is obtrusive, as it requires skin contact via electrodes, chest straps, finger clips, etc. These measurements are not only uncomfortable for the subject, but in some cases (e.g., pulse oximetry) can also restrict activities of daily living. Contactless physiological sensing, that is, remotely measuring vital parameters without electrodes affixed to the patients' skin, can provide a viable solution to these problems. Contactless sensors offer an added advantage because they eliminate the possibility of motion artifacts that may occur with electrode measurements.

In this paper, we explore whether remote measurements of pupillary dilation may be used to estimate heart rate variability. Spontaneous fluctuations in pupillary diameter (SFPD) have been shown to occur in synchrony with autonomic rhythms [3, 4], and pupillary contraction and dilation are known to be under control of the two autonomic branches, which also drive heart rate variability [5]. However, to our knowledge there are no previous reports on estimating SFPDs remotely, as is needed for contactless measurement. It is also unclear whether SFPDs are robust under different ambient illumination levels, which are unavoidable in practical settings. We set to answer these questions by using a desktop eye-tracker to image the eyes remotely. Then, we use the Viola-Jones object-detection algorithm [6] to locate the eyes in the image and a integro-differential operator [7] that is robust to eyelid occlusions to extract pupil and iris centers and radii. This results in a time series of pupil diameters, from which we estimate HRV in the spectral domain. Our results show statistically significant correlations between contactless measurement of SFPDs and ground truth measurements of HRV from a commercial heart rate monitor. We also illustrate the accuracy of the method under different levels of ambient illumination, to which measures of pupil dilation are otherwise very sensitive.

The rest of the paper is organized as follows. Section II provides a brief overview of HRV and pupillometry, and summarizes past work on contactless measurement of physiological variables. Section III presents our image and signal processing approach to contactless measurement of HRV from remote pupillary imaging. Section IV describes the experimental protocol used to validate the method. Data analysis and results are presented in Section V. The paper then concludes with a discussion and directions for future work in Section VI.

II. BACKGROUND AND PRIOR WORK

Heart rate variability (HRV) is the physiological phenomenon of variation in the beat-to-beat (R-R) intervals. It is one of the most widely used quantitative markers of cardiovascular regulation by the autonomic nervous system (ANS). Analysis of HRV can provide important information in the diagnosis of cardiac and other chronic and acute diseases [2, 8]. HRV measures are also widely used in psychophysiology as an indicator of autonomic balance: activation of the sympathetic nervous system (SNS) branch leads to reduction in HRV (fight/flight response), while activation of the parasympathetic nervous system (PNS) component is associated with increases in HRV [1, 2, 8].

978-0-7695-5048-0/13 $26.00 © 2013 IEEE
DOI 10.1109/ACII.2013.38

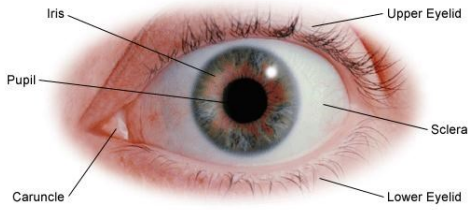

Figure 1: Surface description of the human eye.

Illustrated in Figure 1, the pupil is an aperture in the iris that regulates the amount of light entering the eye. Pupil size can be affected by two factors: optical responses and fluctuations caused by autonomic regulation. The optical response comprises of light reflex, which controls the diameter of the pupil in response to illumination levels, and the accommodation response, which changes the curvature of the lens to control the depth of field. In turn, activation and inhibition of the two ANS branches lead to small-scale spontaneous pupillary fluctuations known as hippus [9]; these fluctuations are the target of our study.

A. Prior work on contactless measurement of physiological variables

Various approaches have been developed for contactless physiological sensing, including radar-based sensors, thermal imaging and, more recently, web and mobile cameras [10-16]. In early work, Grenecker [10] presented an active sensing technique for noncontact measurement of breathing rate. The author used Doppler-modulated radar to sense the shock wave reflecting off the chest wall expansion and contraction during breathing. More recently, Droitcour [11] developed a low-power sensor for measuring cardio-respiratory rates using microwave Doppler radar. This work focused on the circuit specifications of the single-chip Doppler radar for detecting skin surface motion due to heartbeat of the subjects. In related work, Suzuki et al. used an off-the-shelf microwave radar to measure cardiac parameters during arithmetic tasks [12]. These radar-based methods rely on detecting small skin/organ displacements resulting from cardiopulmonary pulses, so they are rather sensitive to motion artifacts. As an example, seemingly small body motion can produce much larger Doppler-modulated radar cross-sections than those caused by the physiological motion of interest. Pavlidis and colleagues have used high-end thermal imaging cameras to measure a variety of physiological variables, including vessel blood flow, cardiac pulse, breathing rate [13]; their methods have been used for large-scale screening in homeland security applications [14, 15]. Recently, Poh et al. [16] have used consumer web cameras for non-contact measurement of HR, breathing rate, and HRV. The authors showed how fluctuations in the RGB color channels of facial images correlate with various physiological variables.

Pupillometry has been widely used in medical and psychophysiology studies. In early work, Ohtsuka et al. [17] found correlation between respiration and fluctuations in pupil diameter. Nakayama et al. [18] performed frequency analysis on the pupillary response and eye movements to study the effect of mental workload. Their study showed a significant increase in power spectral density (0.1–0.5 Hz) with task difficulty. The transient pupil light reflex (PLR) has been used to assess autonomic function in athletes, autistic and healthy children [19-21]. PLR refers to the change in the pupillary size in response to a transient light stimulus under constant illumination. PLR parameters include reflex amplitude, reflex velocity, pupil redilation time, and constriction and redilation velocity. Fan et al. [19] compared the PLR profiles between autistic children and children with typical development. They found autistic group to have significantly longer PLR latency.

These previous studies, however, require controlled measurement setups; as an example, the transient PLR studies in [19-21] used a binocular device with look-through ports and a chinrest, while other pupillometry studies [17, 18] have used head mounted devices. In contrast, we use a non-invasive and non-contact method for pupillary measurements.

III. METHODS

An overview of our approach for contactless measurement of heart-rate variability is illustrated in Figure 2. In a first step, we image the eye region using an IR-based eye tracker, then localize the eyes using the Viola-Jones multi-scale object detector [6]. This detector uses Haar-like features to encode details, which are then used with a cascade of classifiers to locate the presence of the target object (eye) in the given image. Once the eye has been located, we preprocess the image to remove corneal reflections (explained later). Next we detect the pupil-iris boundary using an integro-differential operator, which allows us to compute the pupil diameter. In a final step, we perform spectral analysis of the fluctuations in pupil diameter to extract an index of HRV.

The critical step in the process is accurately detecting the pupil and iris center and their respective boundaries. These are

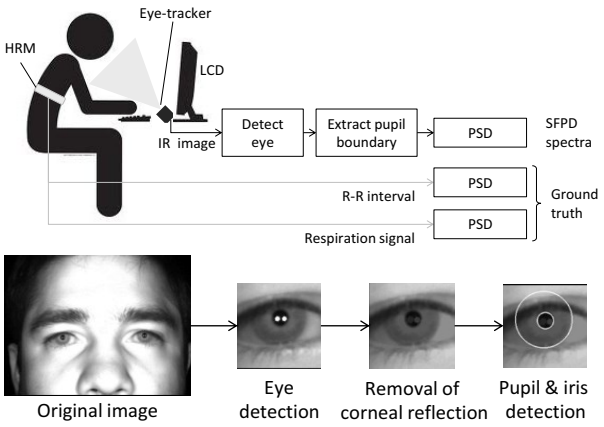

Figure 2: (a) Experimental setup and the steps in computing HRV from pupillary (contactless) and cardiac data (contact-based heart rate monitor (HRM)). (b) Overview of the image processing steps.

challenging problems because of issues such as occlusion by the eye lids and eye lashes, corneal reflections, color of the eye, imaging angle, etc. [22]. A few approaches have been developed for this purpose, which mainly use variants of Hough transform and active contours [23, 24]. Methods based on the Hough transform require tuning of the threshold values for edge detection, which can lead to failures with off-axis and noisy images. Similarly, active contour models can lead to false contours because of eyelids and eyelashes [24].

To address the limitations of conventional methods for iris detection, we use a method originally proposed by Daugman [7] that is robust to occlusions caused by the upper and lower eyelids. The algorithm assumes the pupil and iris have circular geometry, and uses an integro-differential operator to locate the boundaries between them:

$$\{r, x_0, y_0\} = \underset{r,x_0,y_0}{\operatorname{argmax}} \left| G_\sigma(r) * \frac{\partial}{\partial r} \oint_{r,x_0,y_0} \frac{I(x,y)}{2\pi r}\, ds \right| \qquad (1)$$

where $I\,(x, y)$ is the image and $G_\sigma(r)$ is a smoothing gaussian kernel with scale σ. The three parameters: x_0, y_0 (center) and r (radius) define the path of the contour for integration.

Eq. (1) acts as a circular edge detector and it iteratively searches for a maximum contour integral derivative with increasing radius of the circular contour. Namely, a circular projection is obtained at every location of the eye image, and the differential value of the projection is computed. The differential values are then convolved with the gaussian kernel $G_\sigma(r)$ for smoothing. The circular contour with maximum change in pixel intensity results in the largest convolved differential value and is taken as the estimated boundary.

To locate the iris and pupil, the scale parameter σ in the smoothing gaussian kernel takes two distinct values. In a first step, the operator uses a coarse value to find the pronounced boundary between the iris and the sclera. Detecting the iris-sclera boundary considerably reduces the region-of-interest (ROI) for locating the pupil-iris boundary, which requires a much finer spread parameter. In the initial search for the iris-sclera boundary, the angular range of the contour integration in eq. (1) is restricted to two opposing cones of 90° with respect to the horizontal axis of the eye; see Figure 3. This adds robustness to occlusions caused by the eyelids and also reduces the search space.

For computational efficiency, we interchange the order of differentiation and convolution in eq. (1) and concatenate them. To discretize eq. (1), we then use the finite difference approximation of the derivative operator:

$$\frac{\partial G_\sigma(r)}{\partial r} \cong \frac{1}{\Delta r} G_\sigma(n\Delta r) - \frac{1}{\Delta r} G_\sigma((n-1)\Delta r) \qquad (2)$$

then we replace the convolution and integral with summations resulting in eq. (3) (shown below). In eq. (3), Δr is a small

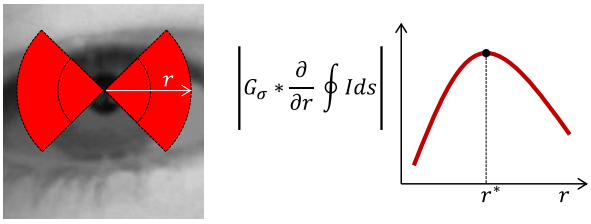

Figure 3: The iris sclera boundary is found by searching for the radius r with largest output in the integro-differential operator

increment in the radius, $\Delta\theta$ is the angular sampling interval along the circular arcs, K is the convolution shift parameter, and $(k\Delta r\ \cos(m\Delta\theta) + x_0),\ k\Delta r\ \sin(m\Delta\theta) + y_0)$ represents a point on the circular contour.

Although this algorithm is a robust technique for pupil detection, it can be susceptible to corneal specular reflections. To address this issue we add a preprocessing step to first detect the reflections as holes and then fill them using a flood-fill operation. This operation brings the intensity of the light area that are surrounded by darker areas up to the same intensity level as the surrounding pixels. This leads to removal of regional extremums that are not connected to image border.

IV. Experiments

To validate our methods, we used a low-cost eye tracking system with IR illumination (easyGaze; Design Interactive, Inc.) [25]. The eye-tracker consists of an IR sensitive camera (resolution 1280×960, 16 FPS) and arrays of IR LEDs (power: 1 mW/cm^2, wavelength: 850 nm) which are offset from the optical axis. The off-axis setup causes the IR light reflection to be projected away from the camera; this makes the pupil darker than the iris and the sclera lighter than the iris, thus enabling accurate segmentation of the pupil and iris boundaries. We also used a Zephyr Bioharness BT chest strap heart rate and breathing sensor [26] (sampling rate: 18 Hz) to obtain ground-truth measures of HRV and respiration.

Before doing spectral analysis, we preprocess the pupillary and cardiac signals to address irregular and burst sampling. As occurrences of R-wave are not equidistantly timed events, this results in irregularly sampled R-R interval time series, which cannot be used directly for spectral analysis. For this reason, we perform bicubic interpolation on the signal to resample it into a uniformly timed series. Similarly we interpolate the pupillary time series to account for missing frames and non-uniform sampling. After resampling, we compute pupil dilation by subtracting the current pupil diameter from a baseline value, measured as the average pupil diameter computed over the past 1.5 seconds using a sliding window. We chose this duration because it is a good approximation of the response time of the pupil to a stimulus [1].

$$\{n\Delta r, x_0, y_0\} = \underset{n\Delta r,x_0,y_0}{\operatorname{argmax}} \left| \frac{1}{\Delta r} \sum_k \left\{ \left(G_\sigma\big((n-k)\Delta r\big) - G_\sigma\big((n-k-1)\Delta r\big) \right) \sum_m I[k\Delta r\ \cos(m\Delta\theta) + x_0),\ k\Delta r\ \sin(m\Delta\theta) + y_0)] \right\} \right| \qquad (3)$$

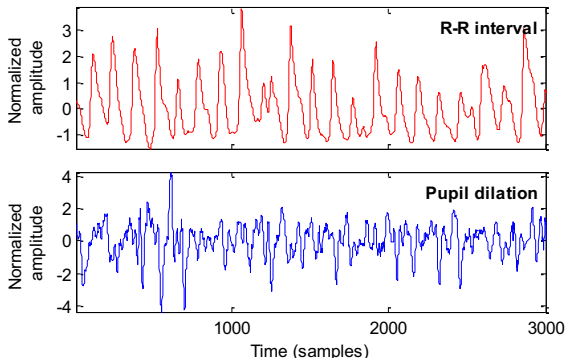

Figure 4: R-R interval and pupil dilation time series

A. Protocol

The study was conducted on 5 subjects, all male, between the ages of 22-28 years. We received approval by the Institutional Review Board and consent from the participants was received before the session. The experiments were performed indoors with participants seated on an adjustable chair in front of the remote eye tracker at a distance of approximately 2 feet. Figure 2 illustrates our experimental setup.

Experiments were divided into two phases. In the first phase, participants were asked to perform paced breathing at 6, 9, 12 breaths per minute (bpm) as well spontaneous breathing. For paced breathing, we used an audio pacing signal which guided the subjects to inspire/expire at appropriate times to maintain the desired breathing pace. For spontaneous breathing, no pacing signal was used, i.e., subjects were asked to breathe at their own pace. Pupillary, cardiac, and breathing data was collected for 5 minutes under each breathing condition for. During this phase the illumination level was kept constant.

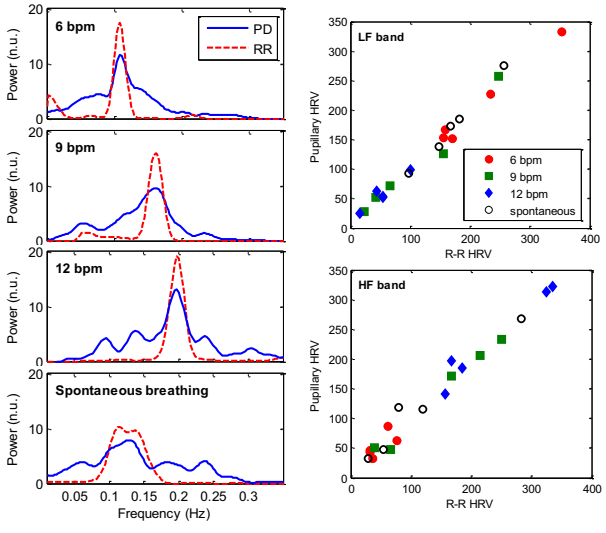

(a) (b)

Figure 5: (a) Power spectra of R-R interval, and pupillary fluctuations for different breathing rates (1 subject). (b) HRV from pupil and R-R for all subjects.

In the second phase, we evaluated our method under two illumination levels (high and low) set by modifying the brightness and color of two 22" LCD monitors placed at a distance of 3 feet from the subject. For the high illumination condition both screens displayed white color at maximum brightness, whereas for the low illumination condition they displayed a black color with minimum brightness. During phase two, participants were asked to follow a 9 bpm breathing pacing signal.

V. Data Analysis and Results

As pupillary fluctuations and R-R interval are both influenced by ANS activity, we hypothesized a strong correlation between the two signals. Analysis in the temporal domain, however, does not reveal any obvious correlation between the two signals –see Figure 4. As a result, using time-domain measures of HRV such as RMSSD (root mean square of the successive differences) to analyze pupillary dilation (PD) is likely to be ineffective [2]. Instead, our method focuses on HRV measures based on frequency-domain analysis. Figure 5 shows the power spectral density (PSD) of the two signals under different breathing paces (6, 9, 12 bpm) and under spontaneous breathing in normalized units (n.u.). Under paced breathing –Figure 5(a), each signal (RR interval: red; PD: blue) shows a prominent peak at the specified breathing rates. The pupillary PSD, however, shows a broader spectral peak; this result is to be expected given the higher noise levels shown in the time-domain signal of pupil dilation in Figure 4. Under spontaneous breathing –Figure 5(a) bottom, both signals also have a much wider spectral spread compared to the paced breathing condition. This result is also reasonable since under spontaneous breathing the breathing rate for each subject changes over time. Overall, though, these plots show that during both paced and spontaneous breathing, there is significant overlap between the RR and PD spectra, which indicates that the PD spectra can be used to compute HRV.

To verify our visual inspection of the results in Figure 5(a), we extracted two spectral features of HRV from both signals: energy in the LF (0.04 to 0.15 Hz) band and in the HF (0.15 to 0.4 Hz) bands. Results are shown in Figure 5(b). The x-axis of the scatter plots represents the HRV features from the heart rate monitor that serves as ground truth, while the y-axis shows the HRV obtained from the contactless method (pupil dilation). A strong correlation between the two measures is evident in both bands. The correlation coefficient between the estimated HRV and ground truth was found to be $r = 0.98$ for the LF and $r = 0.97$ for the HF band ($p < 0.001$ in both cases).

A. Robustness to illumination intensity

Pupillary size is highly sensitive to ambient light intensity. As a result, psychophysiological variables derived from the absolute pupil diameter (e.g., mental workload) must be measured under controlled lighting conditions. However, because our approach relies on fluctuations in pupil diameter

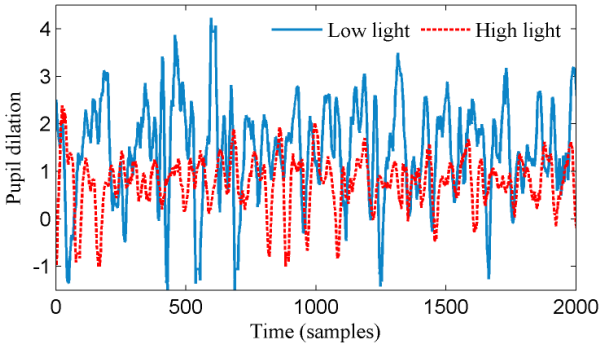

Figure 6: Pupil dilation in low and high light for 1 subject.

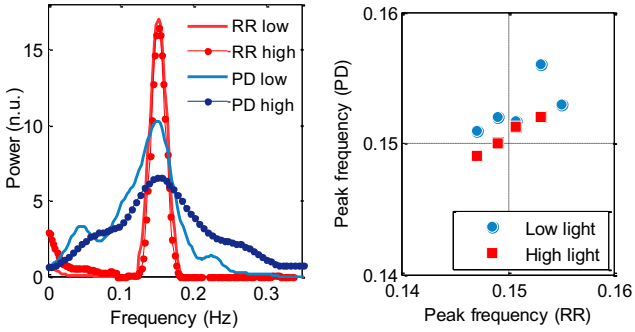

Figure 7: (a) Power spectra of RR interval (RR) and pupil dilation (PD) in Low and high light (1 subject). (b) Peak frequency of RR and PD spectra in L and H light (5 subjects)

as opposed to absolute pupil diameter we hypothesized that it would be robust to lighting conditions.

Figure 6 shows the time-domain signal for pupillary size (one subject) under the low and high illumination conditions described in the Experiment section. With high illumination, the average pupil diameter is reduced to limit the amount of light entering the eye; in contrast, with low illumination, the pupil diameter becomes larger to allow more light. Clearly, any measure relying on absolute pupillary size will have to account for changes in ambient light intensity. Moreover, Figure 6 indicates that ambient light affects not only the average pupil diameter but also the amplitude of the fluctuations. Notice how the fluctuations have lower amplitude under high illumination; this is because under high illumination the pupil is already constricted to a small radius. Thus, a time-domain measure of HRV (e.g., RMSSD) would also be ineffective unless it accounts for changes in lighting.

Figure 7(a) shows the power spectra of the RR interval and PD at high and low illumination levels –same subject as in Figure 6. At both illumination levels, the power spectra shows a peak at 0.15 Hz, which corresponds to the nominal breathing rate of 9 bpm. Thus, while the average pupil dilation and the amplitude of its fluctuations are affected by illumination levels, the frequency of those oscillations remains constant. As observed in the time-domain signals of Figure 6, the peak in the PD power spectra has lower amplitude for the high illumination condition than for the low illumination condition. This suggests that spectral analysis of PD fluctuations is robust to changes in illumination levels. To corroborate this conclusion, Figure 7(b) shows the peak frequency for the RR and PD spectra under the two illumination levels for the five subjects in our study. Regardless of illumination conditions as well as individual differences across subjects, the spectra peaks at around 0.15 Hz, which corresponds to the specified breathing rate of 9 bpm.

VI. Concluding Remarks

We have presented proof-of-concept for the contactless measurement of heart rate variability from spontaneous fluctuations in pupillary diameter. Our method uses IR imaging of the eye combined with an integro-differential operator to measure pupillary fluctuations. Heart rate variability is then computed from the power spectrum of the time-series of pupillary diameters. Our results show a statistically significant correlation between the HRV measurements made from the pupillary spectrum and ground truth values under a range of breathing conditions.

A weakness of pupillary measures is their dependence on illumination levels; the pupillary light reflex is a major component in the overall pupillary response and is known to be larger in magnitude than spontaneous pupillary fluctuations caused by autonomic regulation [1]. For this reason, we also evaluated our measure under the effect of lighting conditions. Our results show that, in contrast with measures based on the absolute pupil diameter or the amplitude of its fluctuations, measures based on the frequency of the fluctuations (such as ours) are robust under different illumination conditions. It should also be noted that the current system has lower sampling rate than required for clinical applications (>250 hz) [2, 16]. However this can be addressed by using cameras with relatively higher framerates.

A. Future work

The next logical step in this research is to extend the method to handle transient changes in ambient illumination. Filtering techniques may be used for this purpose provided that the frequency band of changes in illumination does not overlap with the autonomic rhythms. More elaborate methods may be required in the general case. As an example, our method could be integrated with pupil light reflex models to describe the changes in the pupil diameter as a function of the ambient lighting usig non-linear delay differential equations [27]. Alternatively, a history-dependent point process model of R-R intervals [28] may be used to express the pupillary response as a probabilistic function of ambient lighting and cardio-pulmonary parameters. From this model, we would then extract instantaneous estimates of HRV under transient illumination conditions.

Our results show that the method works well under minor head movements, but additional work is required to test the pupil detection algorithm under larger movements as well as camera

rotations. Despite the use of a coarse-to-fine strategy for the scale parameter σ, our current implementation is computionally expensive because it performs exhaustive search over all values of the radius in the ROI. More efficient methods such as the Adaboost-cascade iris detector suggested by He at al. [22] may be used to improve run time.

In this work we sought to demonstrate the feasibility of measuring heart rate variability from pupillary fluctuations in a contactless fashion. Our method was validated on a relatively small sample size, so extensive trials would be required to ascertain its clinical validity and reliability. Beyond clinical applications, our method may find application in other areas such as biofeedback games, stress assessment and monitoring, human factor studies, and psychophysiological studies. With eye trackers, we can extract point of gaze information which provides rich contextual information. This in corroboration with the measured HRV can be utilized for numerous affective computing applications such as emotion classification, human computer interaction etc. However, we should note that our approach is in no way limited to eye trackers (the remote eye-tracker in our study was used merely as an IR imaging device) and could be combined with inexpensive consumer products such as IR webcams for night vision [29, 30] with minor modifications of conventional webcams [31].

ACKNOWLEDGMENT

This publication was made possible by NPRP grant # 5-678-2-282 from the Qatar National Research Fund (a member of Qatar Foundation). The statements made herein are solely the responsibility of the authors.

REFERENCES

[1] J. T. Cacioppo, L. G. Tassinary, and G. G. Berntson, *Handbook of psychophysiology*: Cambridge University Press, 2007.

[2] "Heart rate variability: standards of measurement, physiological interpretation and clinical use. Task Force of the European Society of Cardiology and North American Society of Pacing and Electrophysiology," *Circulation,* vol. 93, pp. 1043-65, 1996.

[3] G. Calcagnini, S. Lino, F. Censi, and S. Cerutti, "Cardiovascular autonomic rhythms in spontaneous pupil fluctuations," in *Computers in Cardiology 1997*, 1997, pp. 133-136.

[4] G. Calcagnini, F. Censi, S. Lino, and S. Cerutti, "Spontaneous fluctuations of human pupil reflect central autonomic rhythms," *Methods of Information in Medicine-Methodik der Information in der Medizin,* vol. 39, pp. 142-145, 2000.

[5] S. Usui and Y. Hirata, "Estimation of autonomic nervous activity using the inverse dynamic model of the pupil muscle plant," *Annals of biomedical engineering,* vol. 23, pp. 375-387, 1995.

[6] P. Viola and M. Jones, "Rapid object detection using a boosted cascade of simple features," in *Proceedings of the IEEE Computer Society Conference on Computer Vision and Pattern Recognition. CVPR 2001.* , 2001, pp. I-511-I-518 vol. 1.

[7] J. G. Daugman, "High confidence visual recognition of persons by a test of statistical independence," *IEEE Transactions on Pattern Analysis and Machine Intelligence,* vol. 15, pp. 1148-1161, 1993.

[8] J. F. Thayer, S. S. Yamamoto, and J. F. Brosschot, "The relationship of autonomic imbalance, heart rate variability and cardiovascular disease risk factors," *International journal of cardiology,* vol. 141, pp. 122-131, 2010.

[9] I. Loewenfeld and O. Lowenstein, "The light reflex," *The Pupil: Anatomy, Physiology and Clinical Applications,* pp. 189-193, 1993.

[10] E. Greneker, "Radar sensing of heartbeat and respiration at a distance with applications of the technology," in *In Radar 97 (Conf. Publ. No. 449)*, 1997, pp. 150-154.

[11] A. D. Droitcour, "Non-contact measurement of heart and respiration rates with a single-chip microwave Doppler radar," Citeseer, 2006.

[12] S. Suzuki, T. Matsui, S. Gotoh, Y. Mori, B. Takase, and M. Ishihara, "Development of non-contact monitoring system of heart rate variability (hrv)-an approach of remote sensing for ubiquitous technology," *Ergonomics and Health Aspects of Work with Computers,* pp. 195-203, 2009.

[13] M. Garbey, N. Sun, A. Merla, and I. Pavlidis, "Contact-free measurement of cardiac pulse based on the analysis of thermal imagery," *IEEE Transactions on Biomedical Engineering,* vol. 54, pp. 1418-1426, 2007.

[14] I. Pavlidis, N. L. Eberhardt, and J. A. Levine, "Seeing through the face of deception," *Nature,* vol. 415, pp. 35-35, 2002.

[15] P. Buddharaju, J. Dowdall, P. Tsiamyrtzis, D. Shastri, I. Pavlidis, and M. Frank, "Automatic thermal monitoring system (ATHEMOS) for deception detection," in *IEEE Computer Society Conference on Computer Vision and Pattern Recognition*, 2005, p. 1179.

[16] M. Z. Poh, D. J. McDuff, and R. W. Picard, "Advancements in noncontact, multiparameter physiological measurements using a webcam," *IEEE Transactions on Biomedical Engineering,* vol. 58, pp. 7-11, 2011.

[17] K. Ohtsuka, K. Asakura, H. Kawasaki, and M. Sawa, "Respiratory fluctuations of the human pupil," *Experimental Brain Research,* vol. 71, pp. 215-217, 1988.

[18] M. Nakayama and Y. Shimizu, "Frequency analysis of task evoked pupillary response and eye-movement," in *Proc of the symposium on Eye tracking research & applications.* , 2004, pp. 71-76.

[19] X. Fan, J. H. Miles, N. Takahashi, and G. Yao, "Abnormal transient pupillary light reflex in individuals with autism spectrum disorders," *Journal of autism and developmental disorders,* vol. 39, pp. 1499-1508, 2009.

[20] J. A. Capão Filipe, F. Falcao-Reis, J. Castro-Correia, and H. Barros, "Assessment of autonomic function in high level athletes by pupillometry," *Autonomic Neuroscience,* vol. 104, pp. 66-72, 2003.

[21] K. C. Donaghue, M. Pena, A. Fung, M. Bonney, N. Howard, M. Silink*, et al.*, "The prospective assessment of autonomic nerve function by pupillometry in adolescents with type 1 diabetes mellitus," *Diabetic medicine,* vol. 12, pp. 868-873, 1995.

[22] Z. He, T. Tan, Z. Sun, and X. Qiu, "Toward accurate and fast iris segmentation for iris biometrics," *IEEE Transactions on Pattern Analysis and Machine Intelligence,* vol. 31, pp. 1670-1684, 2009.

[23] R. P. Wildes, J. C. Asmuth, G. L. Green, S. C. Hsu, R. J. Kolczynski, J. Matey*, et al.*, "A system for automated iris recognition," in *Proceedings of the Second IEEE Workshop on Applications of Computer Vision, 1994*, 1994, pp. 121-128.

[24] N. Ritter, R. Owens, J. Cooper, and P. P. Van Saarloos, "Location of the pupil-iris border in slit-lamp images of the cornea," in *Proceedings. International Conference on Image Analysis and Processing, 1999.* , 1999, pp. 740-745.

[25] *EasyGaze Eyetracker*. Available: http://designinteractive.net/?p=517

[26] *Bioharness Zephyr 3*. Available: http://www.zephyr-technology.com/products/bioharness-3/

[27] V. F. Pamplona, M. M. Oliveira, and G. V. G. Baranoski, "Photorealistic models for pupil light reflex and iridal pattern deformation," *ACM Transactions on Graphics,* vol. 28, p. 106, 2009.

[28] R. Barbieri, E. C. Matten, A. R. A. Alabi, and E. N. Brown, "A point-process model of human heartbeat intervals: new definitions of heart rate and heart rate variability," *American Journal of Physiology-Heart and Circulatory Physiology,* vol. 288, pp. H424-H435, 2005.

[29] (2012). *GE Wireless Camera with Night Vision*. Available: http://amzn.com/B0013V58WK

[30] (2012). *Agama webcam*. Available: http://www.agamazone.com/products_v1325r.html

[31] C. H. Morimoto, D. Koons, A. Amir, and M. Flickner, "Pupil detection and tracking using multiple light sources," *Image and vision computing,* vol. 18, pp. 331-335, 2000.